

FULL PAPER

Design, synthesis, characterization and biological studies of copper (II) complexes with 2-aminobenzimidazole derivatives as biomimetic agents

J. Joseph* | A. Suman | Nisha Balakrishnan

Department of Chemistry, Noorul Islam Centre for Higher Education, Kumaracoil – 629 180, Tamil Nadu, India

Correspondence

J. Joseph Department of Chemistry Noorul Islam Centre for Higher Education, Kumaracoil – 629 180 Tamil Nadu, India.

Email: josephniche@gmail.com

Four novel copper(II) complexes of 2-aminobenzimidazole derivatives (obtained from the Knoevenagel condensation of acetylacetone (obtained from acetylacetone and halogen-substituted benzaldehydes) and 2-aminobenzimidazole) were synthesized. They were characterized using elemental analysis, molar conductance measurements, and fast atom bombardment mass, Fourier transform infrared, NMR, UV–visible and electron paramagnetic resonance spectroscopies. On the basis of the spectral studies, a distorted square planar geometry was assigned for all the complexes. The antibacterial screening of the ligands and their complexes revealed that all the complexes had higher activities than the free ligands. Superoxide dismutase and antioxidant activities of the copper complexes were also studied. The shifts in ΔE_p , $E_{1/2}$, I_{pc} and I_{pa} values were explored for the interaction of the complexes with calf thymus DNA using the electrochemical technique.

KEYWORDS

Antimicrobial, antioxidant, complexes, DNA binding, Schiff base

1 | INTRODUCTION

β -Diketones have attracted a lot of interest due to their importance as good ligands for chelation with metals and as intermediates in the core of heterocyclic systems such as flavones, benzodiazepine, pyrazole, isoxazole and pyrimidine. They are well known to show keto–enol tautomerism.^[1–7] β -Diketone ligands are considered to have potential due to their enolizing ability.^[8,9] For the purpose of varying the pharmacological activities of β -diketones, we decided to synthesize a series of novel β -diketone derivatives. Transition metal complexes containing β -diketone ligands are commonly found in biological media and play important roles in processes such as catalysis of drug interactions with biomolecules. Metal complexes of β -diketone derivatives have been prepared that show good biological activities. Recently, synthesized Cu(II), Ni(II), Co(II) and Zn(II) complexes were shown to have a broad spectrum of biological activities, motivating researchers in the field of coordination

chemistry of these metal ions.^[10–14] Many biologically active compounds used as drugs possess modified pharmacological and toxicological potentials when administered in the form of metal-based compounds.^[15,16]

In view of the importance of metal complexes, four copper complexes were prepared and characterized and their *in vitro* antibacterial and antifungal properties were investigated. The newly synthesized β -diketones and their metal complexes were characterized using Fourier transform infrared (FT-IR), ¹H NMR, ¹³C NMR and electronic spectroscopies, molar conductance, magnetic moments and elemental analyses. The synthesized ligands (L¹–L⁴) and transition metal chelates have been screened for *in vitro* antibacterial activity against *Staphylococcus aureus*, *Acinetobacter baumannii*, *Escherichia coli* and *Pseudomonas aeruginosa* and for antifungal activity. *In vitro* free radical scavenging activities of the ligands and metal chelates were evaluated using DNA binding and antioxidant assay methods.^[12–14,17–19]

2 | EXPERIMENTAL

2.1 | Materials

All chemicals and solvents were of reagent grade and were purchased from Merck. All supporting electrolyte solutions were prepared using analytical-grade reagents and doubly distilled water. Calf thymus DNA (CT-DNA) was purchased from Genei Biolab, Bangalore, India.

2.2 | Instrumentation

Elemental analyses of ligands and their copper complexes were carried out using a PerkinElmer elemental analyser. Molar conductances of the complexes were measured using a Coronation digital conductivity meter. The ^1H NMR spectra of the ligands were recorded using tetramethylsilane (TMS) as internal standard. Chemical shifts are expressed in units of parts per million relative to TMS. The FT-IR spectra of the ligands and their copper complexes were recorded with a PerkinElmer 783 spectrophotometer in the range 200–4000 cm^{-1} using KBr discs. Electronic spectra were recorded with a Systronics 2201 double-beam UV–visible spectrophotometer in the range 200–800 nm. Magnetic moments were measured using the Guoy method and corrected for diamagnetism of the component using Pascal's constants. Cyclic voltammetry was performed using a CHI 604D electrochemical analyser with a three-electrode system of glassy carbon as the working electrode, a platinum wire as auxiliary electrode and Ag/AgCl as reference electrode. Tetrabutylammonium perchlorate was used as the supporting electrolyte. Solutions were deoxygenated by eradication with nitrogen prior to measurements. The interactions between metal complexes and DNA were studied using electrochemical and electronic absorption techniques. The fast atom bombardment (FAB) mass spectra of ligands and their metal complexes were recorded with a JEOL SX 102/DA-6000 mass spectrometer/data system using argon/xenon (6 kV, 10 A) as the FAB gas. Thermogravimetric analyses were conducted from 0 to 1000°C at a heating rate of 10°C min^{-1} using a PerkinElmer Diamond TG/DTA instrument.

2.3 | DNA binding studies

The binding interactions between the metal complexes and DNA were studied using electrochemical and electronic absorption methods with various concentrations of CT-DNA. Solutions of CT-DNA in 50 mM NaCl/50 mM Tris–HCl (pH = 7.2) gave ratios of UV absorbance at 260 and 280 nm, A_{260}/A_{280} , of ca 1.8–1.9, indicating that the DNA was sufficiently free of protein contamination. The DNA concentration was determined by the UV absorbance at 260 nm after 1:100 dilution. The molar absorption coefficient was taken as 660 $\text{m}^2 \text{mol}^{-1}$. Stock solutions were kept at 4°C and used after not more than four days. Concentrated stock solutions of the complexes were prepared by dissolving them

in dimethylsulfoxide (DMSO) and diluting suitably with the corresponding buffer to the required concentration for all experiments.

2.4 | Absorption titration

Absorption titration experiments were performed by maintaining a constant concentration of the complex while varying the nucleic acid concentration. This was achieved by dissolving an appropriate amount of the copper complex stock solution and by mixing various amounts of DNA stock solutions while maintaining the total volume constant. This resulted in a series of solutions with varying concentrations of DNA but with a constant concentration of the complex. The absorbance (A) of the most red-shifted band of the complex was recorded after each successive addition of CT-DNA. The intrinsic binding constant, K_b , was determined from a plot of $[\text{DNA}]/(\epsilon_a - \epsilon_f)$ versus $[\text{DNA}]$, where $[\text{DNA}]$ is the concentration of DNA in base pairs, ϵ_a the apparent extinction coefficient obtained by calculating $A_{\text{obs}}/[\text{complex}]$ and ϵ_f the extinction coefficient of the complex in its free form. The data were fitted to the following equation where ϵ_b is the extinction coefficient of the complex in the fully bound form:

$$\frac{[\text{DNA}]}{\epsilon_a - \epsilon_f} = \frac{[\text{DNA}]}{\epsilon_b - \epsilon_f} + \frac{1}{K_b(\epsilon_b - \epsilon_f)} \quad (1)$$

Each set of data, when fitted to the above equation, gave a straight line with a slope of $1/(\epsilon_b - \epsilon_f)$ and a y-intercept of $1/K_b(\epsilon_b - \epsilon_f)$. K_b was determined from the ratio of slope to intercept.

2.5 | Antimicrobial activities

The *in vitro* antimicrobial activities of the investigated compounds were tested against bacterial species and fungal species. One day prior to the experiment, the bacterial and fungal cultures were inoculated in broth (inoculation medium) and incubated overnight at 37°C. Inoculation medium containing 24 h grown culture was added aseptically to the nutrient medium and mixed thoroughly to get a uniform distribution. This solution was poured (25 ml in each dish) into Petri dishes and then allowed to attain room temperature. Wells (6 mm in diameter) were cut in the agar plates using appropriate sterile tubes. Then, the wells were filled to the surface of the agar with 0.1 ml of the test compounds dissolved in DMSO (200 mg ml^{-1}). The plates were allowed to stand for an hour in order to facilitate the diffusion of the drug solution. Then the plates were incubated at 37°C for 24 h for bacteria and 48 h for fungi and the diameters of the inhibition zones were measured. Minimum inhibitory concentrations (MICs) were determined using the serial dilution method. The lowest concentration (mg ml^{-1}) of compound that inhibited the growth of bacteria after 24 h

incubation at 37°C and of fungi after 48 h incubation at 37°C was taken as the MIC. The concentration of DMSO in the medium did not affect the growth of any of the microorganisms tested.

2.6 | Synthesis of Knoevenagel condensate β -diketones

A series of Knoevenagel condensate β -diketones with different substituted aromatic aldehydes (3-bromobenzaldehyde, L¹; 3-fluorobenzaldehyde, L²; 3-chlorobenzaldehyde, L³; 3-cyanobenzaldehyde, L⁴) were refluxed in the presence of potassium carbonate as a catalyst in ethanolic medium. The product was formed with loss of water to afford substituted β -diketone. The progress of the reaction was monitored by TLC. After completion of reaction, the reaction mixture was poured on crushed ice. The yellow-coloured Knoevenagel condensate β -diketone was obtained. The separated product was filtered, washed with ice-cold water and dried *in vacuo*.

2.7 | Synthesis of schiff base ligands

A hot ethanolic solution of 2-aminobenzimidazole (2 M) was added dropwise to 1 mol of Knoevenagel condensate β -diketone in the presence of 40 ml of ethanol and refluxed at 42°C with anhydrous potassium carbonate used as a catalyst. The obtained product was set aside in a refrigerator for 12 h. The progress of reaction was monitored by TLC. After completion of reaction the solid material was removed by filtration and recrystallized from ethanol.

Ligand L¹. Molecular formula C₂₆H₂₁N₆Br; molecular weight 497 g mol⁻¹. Yield 68%. Anal. Calcd (%): C, 62.79; H, 4.26; N, 16.89. Found (%): C, 62.54; H, 4.02; N, 16.76. UV (nm): 344, 252. FT-IR (KBr disc, cm⁻¹): 3048–3147 (Ar–H); 2709, 1663 (C=N); 1255 (–NH, benzimidazole moiety). ¹H NMR (CDCl₃, δ , ppm): 7.56–8.56 (m, Ar–H, 12H), 2.51 (1H, s, –CH₃, 6H), 8.6 (–CH=C–, s, 1H), 6.5 (–NH(imidazole), 2H, s). FAB-MS (*m/z*): 498.

Ligand L². Molecular formula C₂₆H₂₁N₆F; molecular weight 436 g mol⁻¹. Yield 72%. Anal. Calcd (%): C, 71.55; H, 4.85; N, 19.25. Found (%): C, 71.32; H, 4.72; N, 19.08. UV (nm): 336, 244. FT-IR (KBr disc, cm⁻¹): 3064–3134 (Ar–H); 2927, 1612 (C=N); 1251 (–NH, benzimidazole moiety). ¹H NMR (CDCl₃, δ , ppm): 7.56–7.84 (m, Ar–H, 12H), 3.51 (1H, s, –CH₃, 6H), 8.2 (–CH=C–, s, 1H), 5.2 (–NH(imidazole), 2H, s). FAB-MS (*m/z*): 437.

Ligand L³. Molecular formula C₂₆H₂₁N₆Cl; molecular weight 453 g mol⁻¹. Yield 60%. Anal. Calcd (%): C, 68.95; H, 4.67; N, 18.55. Found (%): C, 68.72; H, 4.46; N, 18.38. UV (nm): 326, 248. FT-IR (KBr disc, cm⁻¹): 3047–3138 (Ar–H); 2931, 1637 (C=N); 1251 (–NH, benzimidazole moiety). ¹H NMR (CDCl₃, δ , ppm): 7.3–8.5 (m, Ar–H, 12H), 2.5 (1H, s, –CH₃, 6H), 8.7 (–CH=C–, s, 1H), 6.4 (–NH(imidazole), 2H, s). FAB-MS (*m/z*): 454.

Ligand L⁴. Molecular formula C₂₇H₂₁N₇; molecular weight 443 g mol⁻¹. Yield 74%. Anal. Calcd (%): C, 73.13; H, 4.97; N, 22.10. Found (%): C, 72.92; H, 4.68; N, 21.96. UV (nm): 340, 264. FT-IR (KBr disc, cm⁻¹): 3051–3298 (Ar–H); 2931, 1637 (C=N); 1274 (–NH, benzimidazole moiety). ¹H NMR (CDCl₃, δ , ppm): 7.32–8.5 (m, Ar–H, 12H), 2.51 (1H, s, –CH₃, 6H), 8.7 (–CH=C–, s, 1H), 6.5 (–NH(imidazole), 2H, s). FAB-MS (*m/z*): 444.

2.8 | Synthesis of copper complexes

Ethanolic solutions of 2-aminobenzimidazole derivatives (2 M) and copper acetate (1 M) were refluxed for about 6 h at 40°C. The progress of the reaction was monitored by TLC until the product was formed. Then, it was poured on crushed ice. The solid material was removed by filtration and recrystallized from ethanol.

Copper complex of L¹. Molecular formula C₃₀H₂₇N₆O₄BrCu; molecular weight 679 g mol⁻¹. Yield 60%. Anal. Calcd (%): C, 53.07; H, 4.01; N, 12.37; Cu, 9.36. Found (%): C, 52.92; H, 3.86; N, 12.16; Cu, 9.14. UV (nm): 336, 246, 468. FT-IR (KBr disc, cm⁻¹): 3068–3223 (Ar–H); 2899, 1637 (C=N); 1244 (–NH, benzimidazole moiety); 458 (M–O); 551 (M–N); 1413 $\nu_{\text{asy}}(\text{COO}^-)$; 1156 $\nu_{\text{sy}}(\text{COO}^-)$. FAB-MS (*m/z*): 680. $\Lambda_{\text{m}} = 11 \Omega^{-1} \text{ cm}^2 \text{ mol}^{-1}$; $\mu_{\text{eff}} = 1.83 \text{ BM}$.

Copper complex of L². Molecular formula C₃₀H₂₇N₆O₄FCu; molecular weight 618 g mol⁻¹. Yield 64%. Anal. Calcd (%): C, 58.30; H, 4.40; N, 13.59; Cu, 10.28. Found (%): C, 58.05; H, 4.26; N, 13.44; Cu, 10.16. UV (nm): 336, 246, 482. FT-IR (KBr disc, cm⁻¹): 3183–3317 (Ar–H); 2775, 1647 (C=N); 1224 (–NH, benzimidazole moiety); 489 (M–O); 530 (M–N); 1340 $\nu_{\text{asy}}(\text{COO}^-)$; 1274 $\nu_{\text{sy}}(\text{COO}^-)$. FAB-MS (*m/z*): 619. $\Lambda_{\text{m}} = 9 \Omega^{-1} \text{ cm}^2 \text{ mol}^{-1}$; $\mu_{\text{eff}} = 1.80 \text{ BM}$.

Copper complex of L³. Molecular formula C₃₀H₂₇N₆O₄ClCu; molecular weight 635 g mol⁻¹. Yield 60%. Anal. Calcd (%): C, 56.79; H, 4.29; N, 13.24; Cu, 10.01. Found (%): C, 56.58; H, 4.14; N, 13.10; Cu, 9.86. UV (nm): 344, 252, 490. FT-IR (KBr disc, cm⁻¹): 3059–3215 (Ar–H); 2316, 1633 (C=N); 1274 (–NH, benzimidazole moiety); 472 (M–O); 621 (M–N); 1334 $\nu_{\text{asy}}(\text{COO}^-)$; 1166 $\nu_{\text{sy}}(\text{COO}^-)$. FAB-MS (*m/z*): 636. $\Lambda_{\text{m}} = 7 \Omega^{-1} \text{ cm}^2 \text{ mol}^{-1}$; $\mu_{\text{eff}} = 1.85 \text{ BM}$.

Copper complex of L⁴. Molecular formula C₃₁H₂₇N₇O₄Cu; molecular weight 625 g mol⁻¹. Yield 74%. Anal. Calcd (%): C, 59.57; H, 4.35; N, 15.68; Cu, 10.17. Found (%): C, 59.34; H, 4.18; N, 15.52; Cu, 10.04. UV (nm): 340, 266, 480. FT-IR (KBr disc, cm⁻¹): 3102–3160 (Ar–H); 2860, 1760 (C=N); 1264 (–NH, benzimidazole moiety); 462 (M–O); 560 (M–N); 1278 $\nu_{\text{asy}}(\text{COO}^-)$; 1192 $\nu_{\text{sy}}(\text{COO}^-)$. FAB-MS (*m/z*): 626. $\Lambda_{\text{m}} = 6 \Omega^{-1} \text{ cm}^2 \text{ mol}^{-1}$; $\mu_{\text{eff}} = 1.84 \text{ BM}$.

3 | RESULTS AND DISCUSSION

The analytical, physical property and molar conductance data of the complexes are summarized in experimental section. The Cu(II) complexes were dissolved in DMSO and the molar conductivities of 10^{-3} M solutions at room temperature were measured. The low conductance values ($6\text{--}11 \Omega^{-1} \text{cm}^2 \text{mol}^{-1}$) of the complexes support their non-electrolytic nature. Thus, the present complexes have non-electrolytic nature as evidenced by the involvement of acetate ions in coordination. This result is further confirmed from the chemical analysis of CH_3COO^- ion, not precipitated by addition of FeCl_3 . The elemental analysis data of the complexes are in good agreement with theoretical values presented. The results obtained from micro-analytical measurements, metal estimation, conductivity and mass spectral data confirm the stoichiometry of the copper complexes as $[\text{CuL}(\text{OAc})_2]$. The magnetic moments of copper(II) in any of its geometries lies around 1.9 BM which is very close to spin-only value, i.e. 1.73 BM. The values found in our case lie in the range 1.80–1.85 BM. These values are typical for mononuclear copper(II) compounds having d^9 electronic configuration. The observed magnetic moments of all the complexes correspond to distorted square planar Cu(II) complexes. However, the values are slightly higher than the expected spin-only values due to spin-orbit coupling contribution.

3.1 | FT-IR spectra

The FT-IR spectra of $\text{L}^1\text{--L}^4$ and their copper complexes (supporting information) show a band at 1680cm^{-1} for the imine $\nu(\text{C}=\text{N})$ group which results from the Schiff base condensation of 2-aminobenzimidazole and Knoevenagel condensate. It shifts to a lower frequency of 1663cm^{-1} after complexation.^[20] Moreover, the new bands appearing at 466 and 533cm^{-1} correspond to $\nu(\text{M}-\text{N})$ and $\nu(\text{M}-\text{O})$.^[21] Also, the new bands at 1357 and 1255cm^{-1} correspond to symmetric and asymmetric stretching for $\nu(\text{M}-\text{O})$ which evidence the participation of the COO^- ion in the complexes. These facts are further supported by the appearance of bands at $1380\text{--}1465 \text{cm}^{-1}$ and $1255\text{--}1357 \text{cm}^{-1}$ attributed to $\nu_{\text{asy}}(\text{COO}^-)$ and $\nu_{\text{sy}}(\text{COO}^-)$, respectively, for all copper complexes. The difference between $\nu_{\text{asy}}(\text{COO}^-)$ and $\nu_{\text{sy}}(\text{COO}^-)$ in the metal complex spectra is *ca* 100cm^{-1} ($105\text{--}125 \text{cm}^{-1}$) suggesting the mode of coordination of carboxylate group in the copper complexes is monodentate. Finally, it was determined that the copper complexes behave as bidentate and coordinate through azomethine nitrogen atoms and acetate ions.

3.2 | NMR spectra

The ^1H NMR spectra of $\text{L}^1\text{--L}^4$ (supporting information) show a D_2O exchangeable peak at 8.24 ppm as a singlet.

The peaks observed in the range 7.32–7.91 ppm are assignable to the proton of benzene units as multiplet peaks. The chemical shift observed at 7.95 ppm is assigned to the proton of the azomethine groups ($\text{CH}=\text{N}$) as a singlet. The ^1H NMR resonances with the expected integrated intensities are observed as a singlet at 6.30 ppm (1H) for aromatic ethylene proton and as a triplet at 2.32 and 2.57 ppm for the methyl group protons.

The ^{13}C NMR spectra of all the compounds show the signals in the expected regions. The azomethine carbon of the β -diketone derivative is observed in the ligand spectra at 162.6–163.4 ppm. Signals in the range 118.20–128.50 ppm are observed in the spectra of all the compounds due to the aromatic carbons. The signals of carbons $\text{C}=\text{CH}-$ and $\text{C}-\text{CH}-$ of the β -diketone derivatives are observed at 112.6–113.8 and 176.5–177.4 ppm.

3.3 | Mass spectra

The FAB mass spectra of the Schiff bases and their corresponding copper complexes were recorded and compared for their stoichiometry compositions. The $[\text{CuL}^1(\text{OAc})_2]$ complex shows a molecular ion peak at m/z 680. This molecular ion on losing two acetate ions gives a fragment ion peak at m/z 560 and this undergoes demetallation to form the species $[\text{L}]^+$ with a fragment ion peak at m/z 497. Cu complex $[\text{CuL}^2(\text{OAc})_2]$ shows a molecular ion peak (M^+) at m/z 619. Further, the fragmentation of two acetate ions is observed with a peak at m/z 499. After losing the metal, the corresponding ligand ($[\text{L}]^+$) shows a molecular ion peak at m/z 436. The mass spectrum of Cu(II) complex $[\text{CuL}^3(\text{OAc})_2]$ shows a molecular ion peak (M^+) at m/z 636. The second fragmentation of two acetate ions leads to the formation of ligand moiety of 2-aminobenzimidazole with molecular ion peak at m/z 516, and elimination of metal results in an ion peak ($[\text{L}]^+$) at m/z 453. In the case of $[\text{CuL}^4(\text{OAc})_2]$ complex, the molecular ion peak is observed at m/z 626. This molecular ion further loses two acetate atoms giving a fragment ion peak at m/z 506 and undergoes demetallation to form the species $[\text{L}]^+$ giving fragment ion peak at m/z 443. Elemental analysis values are in close agreement with the values calculated from the molecular formulae of these complexes, which is further supported by the FAB-MS data of representative complexes. The mass spectra of L^1 and its copper complex are shown in the supporting information.

3.4 | Electron paramagnetic resonance (EPR) spectra

The X-band EPR spectrum of $[\text{CuL}^4(\text{OAc})_2]$ at 300 K shows an intense absorption at high field. However, this complex in the frozen state shows four well-resolved peaks with low intensities in the low-field region (Figure 1) and one intense peak in the high-field region. The magnetic susceptibility of 1.8 BM indicates that the complex is mononuclear. This is also evident from the absence of a half field signal. Observed

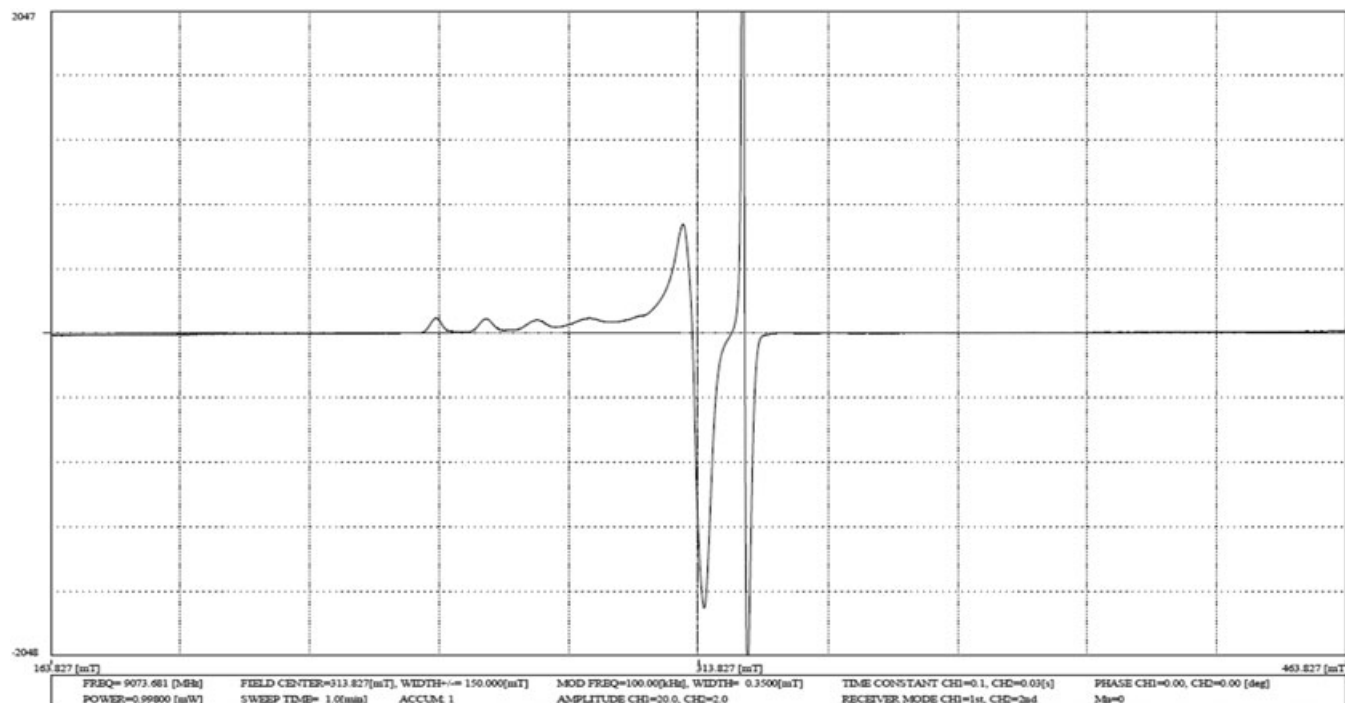


FIGURE 1 ESR spectrum of copper complex of L^1 at 77 K

in the spectrum is a peak at 1600 G due to the $m_s = \pm 2$ transition, ruling out Cu–Cu interactions.^[22]

In square planer complexes, the unpaired electron is in the $d_{x^2-y^2}$ orbital giving $^2B_{1g}$ as the ground state ($g_{\parallel} > g_{\perp} > 2$). From the observed values ($A_{\parallel} = 169 > A_{\perp} = 52$; $g_{\parallel} = 2.34 > g_{\perp} = 2.05 > 2$) it is clear that the ESR parameters coincide well with related square planer system.^[23] In the axial spectrum, the g values related to the exchange interaction are negligible. If the value of G is less than 4, the exchange interaction is considerable. For the present copper complexes, a G value of 6.8 suggests that the tetragonal axes are aligned parallel or slightly misaligned, consistent with $d_{x^2-y^2}$ ground state.

The in-plane σ -bonding covalence parameter α^2 is related to A_{\parallel} , g_{\parallel} and g_{\perp} according to the following equation:

$$\alpha^2 = \frac{A_{\parallel}}{P} + g_{\parallel} - 2.0023 + \frac{3}{7}g_{\perp} - 2.0023 + 0.04$$

A value of $\alpha^2 = 0.5$ indicates covalent bonding, while a value of $\alpha^2 = 1.0$ suggests complete ionic bonding in complexes. The observed value of $\alpha^2 = 0.56$ indicates that the complexes have some covalent character. The out-of-plane π -bonding (γ^2) and in-plane π -bonding (β^2) parameters are calculated from the following expressions:

$$\beta^2 = \frac{g_{\parallel} - 2.0023E}{-8\lambda d^2}$$

$$\gamma^2 = \frac{g_{\perp} - 2.0023E}{-8\lambda d^2}$$

In these equations, $\lambda = -828 \text{ cm}^{-1}$ for the free metal ion. The observed β^2 (1.72) and α^2 (0.56) values indicate that there is interaction in the out-of-plane π -bonding whereas the in-plane π -bonding is complex ionic. This is also confirmed by the orbital reducing factors which are estimated using the following relations:

$$K_{\parallel} = g_{\parallel} - 2.0023 \frac{\Delta E}{8\lambda_0}$$

$$K_{\perp} = g_{\perp} - 2.0027 \frac{\Delta E}{2\lambda_0}$$

where λ_0 is the spin–orbital coupling constant for the copper(II) ion (-828 cm^{-1}) and K_{\parallel} and K_{\perp} are the parallel and perpendicular components of the orbital reduction factor(K), respectively.

Significant information about the nature of bonding in the copper(II) complexes can be derived from the relative magnitudes of K_{\parallel} and K_{\perp} . In the case of pure of σ -bonding, $K_{\parallel} \approx K_{\perp} = 0.77$; whereas $K_{\parallel} < K_{\perp}$ implies considerable in-plane π -bonding; while for out-of-plane π -bonding, $K_{\parallel} > K_{\perp}$. For the present complexes, the observed order is K_{\parallel} (0.96) $>$ K_{\perp} (0.54) implying a greater contribution from out-of-plane π -bonding than from in-plane π -bonding.

These results are anticipated because there are no appropriate ligand orbitals to combine with the d_{xy} orbitals of copper(II) ions. The P values for a complex containing N_2O_2 donor atoms all lie in the range 0.22–0.29 cm^{-1} . The

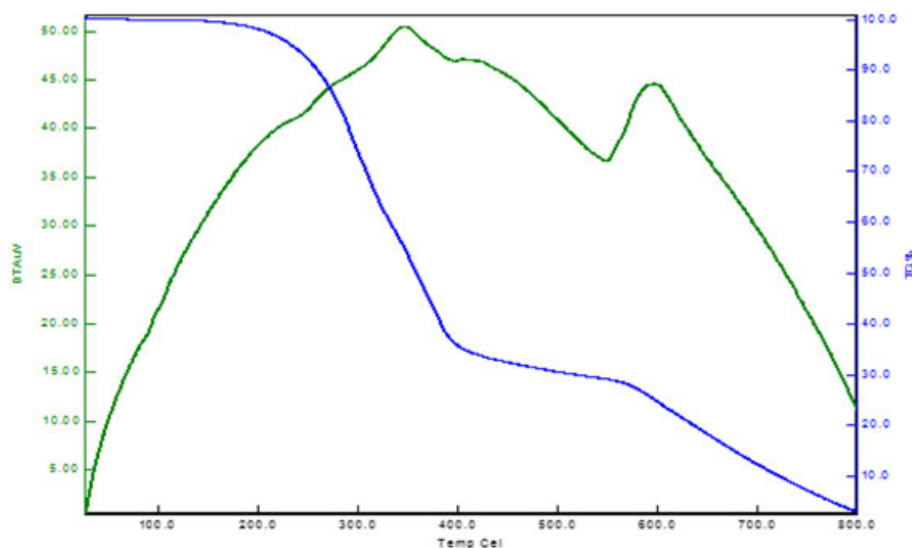


FIGURE 2 Thermogram of copper complex of L^1

P values for the copper complexes are consistent with bonding of copper with nitrogen and oxygen donor atoms.

3.5 | Thermogravimetric analysis

The thermal decomposition behaviour of the complexes $[CuL^1(OAc)_2]$ (Figure 2) and $[CuL^2(OAc)_2]$ was followed up to 1000°C in dynamic nitrogen atmosphere. The correlations between the various decomposition steps of the complexes and the corresponding weight losses are discussed in terms of the proposed formulae of the complexes.

The thermal decomposition pattern of the $[CuL^1(OAc)_2]$ complex displays four steps of weight loss: (i) the weight loss at a relatively low temperature range $190\text{--}360^\circ\text{C}$ is attributed to the removal of the coordinated acetate ions; (ii) elimination of the coordinated 2-aminobenzimidazole ligand is observed with partial decomposition of the parent organic ligand in the range $360\text{--}580^\circ\text{C}$; and (iii) the final decomposition step involves the complete removal of the organic residue in the range $580\text{--}800^\circ\text{C}$ and the formation of the metallic oxide CuO as a final thermal decomposition product. The final weight losses in these cases agree with the formation of the respective metal oxide. The presence of coordinated water molecules in the metal complexes further supports the assumption made on the basis of the FT-IR spectral studies. The final decomposition products were identified using FT-IR spectroscopy with corresponding spectra obtained under the same condition as the acetate and imine groups.

The stability of the obtained copper(II) complexes was investigated kinetically using the Coats–Redfern equation. The results are in the order $[CuL^1(OAc)_2]$, $[CuL^2(OAc)_2]$, $[CuL^3(OAc)_2]$, $[CuL^4(OAc)_2]$. The higher values of activation energies for the elimination of chlorine atoms indicate that they are coordinated with the copper. The relatively high value for the L^2 complex as well as for the L^3

and L^4 complexes indicate that the organic part of the ligand is strongly coordinated with copper(II) ions. This also indicates that the chloro copper(II) complex has a higher thermal stability than the other complexes.

3.6 | DNA studies

DNA as a therapeutic target has attracted researchers to corresponding therapeutic agents. Studies of binding between small molecules and DNA are important and fruitful for developing and designing efficient drugs. Here, CT-DNA was selected as DNA model because of its medical importance, low cost and ready availability to study the probable antimicrobial action mechanism of the compounds at a molecular level using UV–visible spectroscopic and electrochemical methods.

Hypochromism and hyperchromism are very important spectral features for distinguishing the change of DNA double-helical structure in absorption spectroscopy. Due to the interaction between the electronic states of an intercalating chromophore and that of the DNA base, the observed large hypochromism suggests a close proximity of the aromatic chromophore to the DNA bases with a fixed concentration of DNA. UV–visible absorption spectra were recorded with increasing amounts of compound.

3.6.1 | Electronic spectroscopy

In the UV region of the spectra, all the ligands show an absorption band around $312.2\text{--}323.8\text{ nm}$ (due to $\pi\text{--}\pi^*$ transition) and their copper complexes exhibit an intense absorption around $340\text{--}364.5\text{ nm}$. With increasing concentration of DNA, both the ligands and their complexes show hypochromicity and a red-shifted charge transfer peak maxima in the absorption spectra (Figure 3). In the case of the ligands, the change in hypochromicity may be attributed to the nature of the binding of the complexes with DNA, which

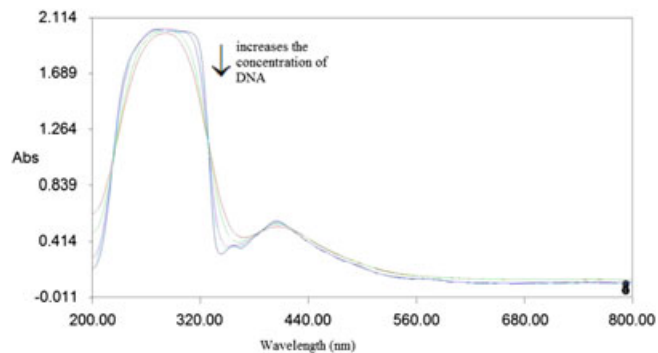


FIGURE 3 Absorption spectra of $[\text{CuL}^1(\text{OAc})_2]$ in the absence and presence of CT-DNA. Arrow shows the absorbance changing with increasing DNA concentration

is significant due to π -stacking or hydrophobic interactions of the aromatic phenyl rings.^[24] The strong binding affinity of the metal complexes is due to additional π - π interaction through the aromatic phenyl rings and central metal ions as compared with Schiff base ligands. From the results, ligands themselves act as weak intercalators as compared to complexes which act as strong intercalators. These results suggest that intercalative ligands with extended aromatic plane, good conjugation effect and electron-withdrawing substituted groups can greatly promote the DNA-binding ability of their Knoevenagel condensate complexes.

3.6.2 | Cyclic voltammetric studies

The cyclic voltammograms of a glassy carbon electrode in solutions containing $[\text{CuL}^1(\text{OAc})_2]$ in the absence and in the presence of varying amounts of DNA are shown in Figure 4. The presence of DNA causes a considerable decrease in the voltammetric current of the redox wave with

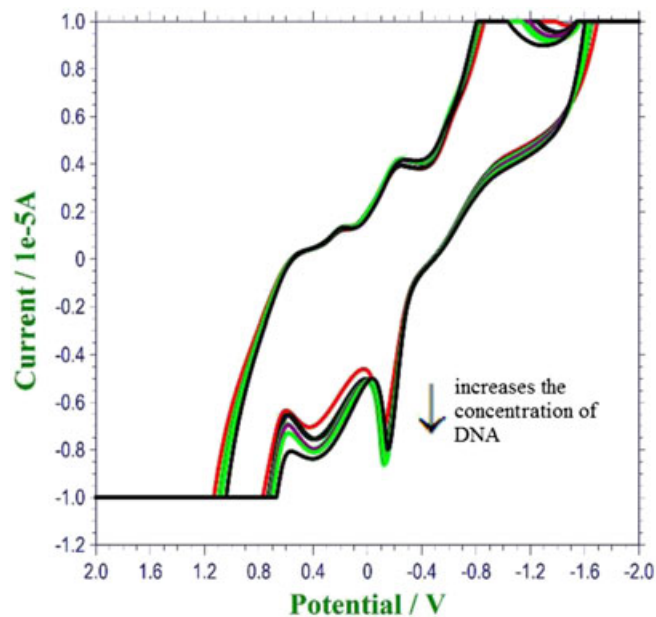


FIGURE 4 Cyclic voltammograms of copper complex of L^1 in the absence (red) and presence (green) of DNA at various concentrations

a slight shift in $E_{1/2}$ to positive potential. The decrease of the voltammetric currents in the presence of DNA may be attributed to slow diffusion of the metal complex bound to CT-DNA. This in turn indicates the extent of binding affinity of the complex to DNA. The net shift in $E_{1/2}$ can be used to estimate the ratio of equilibrium constants for the binding of 2+ and 1+ ions to DNA. The quasireversible redox couples for Cu(II) and Zn(II) complexes in DMF-buffer solution that have been studied upon addition of CT-DNA and the shifts of the cathodic (E_{pc}) and anodic (E_{pa}) potentials. No new redox peaks appear after the addition of CT-DNA to each complex, but the current intensity of all the peaks decreases significantly, suggesting the existence of an interaction between each complex and CT-DNA. The decrease in current intensity can be explained in terms of an equilibrium mixture of free and DNA-bound complexes to the electrode surface.^[25] Finally, the conclusion drawn from the voltammetric study is that the copper complexes can bind to DNA via the intercalative binding mode.

3.7 | Antimicrobial studies

The Schiff bases and their complexes were screened for their *in vitro* antimicrobial activity. The antibacterial activity of the complexes was investigated against both Gram-positive and Gram-negative bacteria using the disc diffusion method. The results indicate that all complexes have a higher antimicrobial activity than the free ligands. This is due to the greater lipophilic nature of the complexes. When the concentration of the complexes increases, the activity also increases. The concentration plays a vital role in increasing the degree of inhibition. The higher antimicrobial activity of the metal complexes compared to ligands may be due to the change in structure on coordination, and chelation tends to make metal complexes act as more powerful and potent bacteriostatic agents, thus inhibiting the growth of bacteria. This increase in the activity of the complexes can be explained on the basis of chelation theory. Chelation considerably reduces the polarity of the metal ion because of partial sharing of its positive charge with donor groups and possible electron delocalization over the whole chelate ring. Such a chelation could enhance the lipophilic character of the central metal atom.

The *in vitro* antimicrobial activities of the investigated compounds were tested against the bacterial species *Acinetobacter baumannii*, *Staphylococcus aureus*, *Escherichia coli*, *Klebsiella pneumoniae* and *Pseudomonas aeruginosa* using the disc diffusion method (Table 1).^[26,27] The inhibitions around the antibiotic discs were measured after incubation and streptomycin was used as a standard drug.

In general, important physicochemical behaviour and structural characteristics that are responsible for the antimicrobial activities are:

TABLE 1 Minimum inhibitory concentration of the synthesized compounds against growth of bacteria ($\mu\text{g ml}^{-1}$)

Compound	<i>Acinetobacter baumannii</i>	<i>Klebsiella pneumoniae</i>	<i>Staphylococcus aureus</i>	<i>Escherichia coli</i>	<i>Pseudomonas aeruginosa</i>
L ¹	28	26	23	24	28
L ²	24	23	25	25	24
L ³	30	21	22	20	30
L ⁴	34	28	32	38	42
CuL ¹ (OAc) ₂	11	10	6	12	7
CuL ² (OAc) ₂	13	9	8	14	9
CuL ³ (OAc) ₂	16	11	6	13	8
CuL ⁴ (OAc) ₂	14	15	7	17	6

- i. lipophilic character permits the passage of molecules to penetrate through the lipid membrane;
- ii. –NH group actively forms hydrogen bonds with constituents in the cell wall and increases the activity;
- iii. the spatial orientation allows a favourable approach of the complexes to interact with biomolecules; and
- iv. the presence of uncoordinated donor atoms permits the detection of sites in the cell wall and enhances the solubility. There are five different modes of bacterial action that have been reported in the literature as follows: (1) distribution of cell wall constituents, (2) inhibition of protein synthesis, (3) inhibition and prevention of replication of nucleic acid, (4) interference of metabolic reactions and (5) breakage of cell wall leading to the apoptosis of microorganisms. The literature indicates that the electrostatic interaction between bacteria and metal complexes leads to better pharmacological activities with different mechanistic actions. Hence, it may be concluded that the antimicrobial activities of the complexes are not only due to chelation but involve other contributions of different structural moieties. This encouraged and motivated much interest to study the interactions of these bioactive compounds with DNA to further explore the possible preliminary mechanism of action and transport behaviour.

3.8 | Antioxidant activity

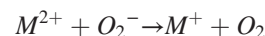
The antioxidant activity of free ligands, complexes and the standard ascorbic acid were assessed on the basis of the radical scavenging effect of the stable DPPH (1,1-diphenyl-2-picrylhydrazyl) free radical. A comparison is made of the antioxidant activity of L¹–L⁴ (IC₅₀ values of 86, 92, 98 and 80 $\mu\text{g ml}^{-1}$) and the copper complexes (IC₅₀ values are 62, 56, 43 and 77 $\mu\text{g ml}^{-1}$). This suggests that the Cu (II) complex of L³ possesses higher scavenging activity towards hydroxyl radical than the parent ligand. The values are found to be close to that of the standard ascorbic acid (IC₅₀ value of 22 $\mu\text{g ml}^{-1}$).

3.9 | Superoxide dismutase (SOD) activity

Superoxide anions have a very short half-life and are produced continuously. In this colorimetric-based assay,

inhibition of the reduction of nitroblue tetrazolium (NBT) to formazan (F) by the metal(II) complexes under investigation was used for detection of the SOD mimetic catalytic activity of these chelates in phosphate buffer under similar biological conditions. The observed IC₅₀ values of the copper complexes of L¹–L⁴ and of native SOD are 0.8, 0.6, 0.4, 0.9 and 0.04 μM , respectively.

The higher SOD activities of copper complexes may be attributed to the flexible ligands, which are able to accommodate the geometric change from Cu(II) to Cu(I) and subsequent changes in the substrate O₂^{•−} into hydrogen peroxide. The mechanism proposed for the dismutation of superoxide anions by both SOD and complexes of L² and L³ is thought to involve redox cycling of metal(II) ions:



It has been proposed that electron transfer between copper(II) and superoxide anion radicals occurs through direct binding. Therefore, the copper complexes exhibit higher SOD activity than other metal complexes. This observation is confirmed by distortion of geometry ('f' factor value). The synthesized copper complexes have higher distortion of geometry.

4 | CONCLUSIONS

The design and synthetic approach was concentrated on the development of copper complexes of β -diketone derivatives with improved biological activity. The low molar conductance values of the complexes correspond to non-electrolytic nature. The antimicrobial screening results indicated the higher potency of the copper complex of β -diketone derivative L³ as compared with the other copper complexes. The improved activities of copper complexes with β -diketone derivatives reported here should open up new opportunities for synthesizing different derivatives around the ' β -diketone' scaffold as antimicrobial agents. On the basis of the observations reported, modification will be done to improve antimicrobial activity. *In vivo* studies of the complexes are in progress in order to understand the variation in their biological effects, which could be helpful in designing more potent antimicrobial agents for therapeutic use.

ACKNOWLEDGMENTS

The authors thank the Science & Engineering Research Board (SERB), DST, New Delhi for financial support. They also express their gratitude to Dr A.P. Majeed Khan, Chancellor, Noorul Islam Centre for Higher Education, Department of Chemistry for providing research facilities.

REFERENCES

- [1] A. S. Rajbhoj, N. S. Korde, S. T. Gaikwad, S. S. Korde, *Pharma Chem.* **2012**, *4*, 1868.
- [2] A. R. Siedle, in *Comprehensive Coordination Chemistry, Vol. 2* (Eds: G. Wilkinson, R. D. Gillard, J. A. McCleverty), Pergamon, Oxford, **1987**, p. 365.
- [3] L. Tang, S. Zhang, J. Yang, W. Gao, J. Cui, T. Zhuang, *Molecules* **2004**, *9*, 842.
- [4] R. Kumar, Y. Joshi, *ARKIVOC* **2007**, *9*, 142.
- [5] T. Dziemboska, Z. Rozwadowski, *Curr. Org. Chem.* **2001**, *5*, 289.
- [6] C. Lin, G. Wei, M. Huang, J. Food Drug, *Anal.* **2005**, *13*, 284.
- [7] G. D. Diana, P. M. Carabateas, R. E. Johnson, G. L. Williams, F. Pancic, J. C. Collins, *J. Med. Chem.* **1978**, *21*, 889.
- [8] N. Acton, A. Brossi, D. L. Newton, M. B. Sporn, *J. Med. Chem.* **1980**, *23*, 805.
- [9] D. Simoni, F. P. Invidiata, R. Rondanin, S. Grimaudo, *Tetrahedron Lett.* **1998**, *39*, 2449.
- [10] O. G. Kuzueva, Y. V. Burgart, V. I. Saloutin, O. N. Chupakhin, *Chem. Heterocycl. Compd.* **2001**, *37*, 1130.
- [11] I. Andrae, A. Bringhen, F. Bohm, H. Gonzenbach, *Chem. Sci. Trans.* **2014**, *3*, 117.
- [12] N. P. Singh, A. N. Srivastava, *Asian J. Chem.* **2013**, *25*, 533.
- [13] C. M. Sharaby, G. C. Mohamed, M. M. Omar, *Spectrochim. Acta* **2007**, *66*, 935.
- [14] M. Sonmez, M. Celebi, I. Berber, *Eur. J. Med. Chem.* **2010**, *45*, 1935.
- [15] S. Tabassum, G. C. Sharma, F. Arjmand, A. Azam, *Nanotechnology* **2010**, *21*, 195.
- [16] A. Arbaoui, C. Redshaw, N. M. Sanchez-Ballester, M. R. J. Elsegood, D. L. Hughes, *Inorg. Chim. Acta* **2011**, *365*, 96.
- [17] S. Tabassum, S. Amir, F. Arjmand, C. Pettinari, F. Marchetti, N. Masciocchi, G. Lupidi, R. Pettinari, *Eur. J. Med. Chem.* **2013**, *60*, 216.
- [18] A. Alagha, L. Parthasrathi, D. Gaynor, H. M. Bunz, Z. A. Starikova, E. Farkas, E. C. O. Brien, M. J. Gil, K. B. Nolan, *Inorg. Chim. Acta* **2011**, *368*, 58.
- [19] K. Zelga, M. Leszczynski, I. Justyniak, A. Kornowicz, M. Cabaj, *Dalton Trans.* **2012**, *41*, 5934.
- [20] N. Chitrapriya, Y. J. Jang, S. K. Kim, H. Lee, *J. Inorg. Biochem.* **2011**, *105*, 1569.
- [21] C. H. Collins, P. M. Lyre, J. M. Grange, *Microbiological Methods*, 6th ed., Butterworth, London **1989**.
- [22] N. Raman, S. Johnson Raja, J. Joseph, J. Chilean, *Chem. Soc.* **2007**, *52*, 1138.
- [23] S. Jone Kirubavathy, R. Velmurugan, K. Parameswari, S. Chitra, *J. Chem. Pharm. Res.* **2015**, *15*, 246.
- [24] N. Shahabadi, S. Mohammadi, *Bioinorg. Chem. Appl.* **2012**, *571*, 913.
- [25] N. Raman, A. Selvan, R. Mahalakshmi, M. Selvaganapathy, J. Iranian, *Chem. Res.* **2012**, *5*, 197.
- [26] J. Gangoue-Pieboji, N. Eze, A. N. Djintchui, B. Ngameni, N. Tsabang, D. E. Pegnyemb, L. Biyiti, P. Ngassam, S. Koulla-Shiro, M. Galleni, *J. Infect. Dev. Countr.* **2009**, *3*, 671.
- [27] S. H. Masood, N. Aslam, *Oman Med. J.* **2010**, *25*, 199.

SUPPORTING INFORMATION

Additional Supporting Information may be found online in the supporting information tab for this article.

How to cite this article: Joseph, J., Suman, A., and Balakrishnan, N. (2016), Design, synthesis, characterization and biological studies of copper(II) complexes with 2-aminobenzimidazole derivatives as biomimetic agents, *Appl. Organometal. Chem.*, doi: 10.1002/aoc.3585